Electronic Research Archive

http://www.aimspress.com/journal/era

ERA, 33(1): 102–120.
DOI: 10.3934/era.2025006
Received: 10 November 2024
Revised: 18 December 2024
Accepted: 03 January 2025
Published: 14 January 2025

Theory article

Chaotic performance and circuitry implement of piecewise logistic-like mapping

Caiwen Chen[1], **Tianxiu Lu**[1,2,*] **and Ping Gao**[1]

[1] College of Mathematics and Statistics, Sichuan University of Science and Engineering, Zigong 643000, China

[2] Sichuan Province University Key Laboratory of Bridge Non-destruction Detecting and Engineering Computing, Zigong 643000, China

* **Correspondence:** Email: lubeeltx@163.com.

Abstract: Discrete chaotic systems are now a meaningful research area due to their intricate dynamical characteristics. This paper introduces a novel piecewise logistic-like mapping chaotic system and rigorously establishes its Devaney chaoticity through mathematical proofs. Experimental findings demonstrate that, compared to the traditional logistic mapping, the logistic-like mapping exhibits more complex dynamic behaviors, such as bifurcation diagram, Lyapunov exponents, permutation entropy, sensitivity, and distribution of function sequences. Furthermore, in order to implement the suggested new chaotic system, a simulation circuit is designed, and a PSIM simulation model is established to validate feasibility of the simulation circuit.

Keywords: chaos; piecewise logistic-like mapping; Devaney chaos; circuit implementation

1. Introduction

In 1976, May introduced several chaotic mappings based on simple mathematical models [1]. Among these, the logistic mappings (LM_S) are notable examples. The logistic mappings are a simple discrete-time dynamic system characterized by its straightforward expression, yet it exhibits a rich array of dynamic behaviors. It has garnered widespread attention in communication systems, pseudo-random sequence generation, neural networks, switching systems, and cryptography. For instance, Buchner et al. [2] proposed a logistic mapping model with delayed feedback. So far, on the basis of one-dimensional logistic mapping, the system of high-dimensional logistic mapping has also attracted wide attention. Tian et al. [3] presented a two-dimensional logistic mapping. Henon et al. [4] proposed a new discrete chaotic system capable of producing curved shapes. Sprott et al. [5] proposed a high-dimensional logistic mapping. Furthermore, Wu et al. [6] proposed a logistic mapping model

with fractional delayed feedback. Wang et al. [7] proposed a piecewise logistic mapping and studied its chaotic properties. Rak et al. [8] introduced a generalized logistic mapping. Sayed et al. [9] studied a collection of four generalized logistic mappings, in which the conventional logistic mapping is a particular instance. Wu et al. [10] introduced a discrete fractional-order logistic mapping in the context of the left Caputo discrete delta calculus. Leonel et al. [11] discussed the dynamical properties of a logistic-like mapping.

Due to the rich dynamic behavior of logistic mappings and logistic-like mappings, there are many applications of them. For example, Pareek et al. [12] proposed a new approach to image encryption based on 80-bit external key and two chaotic logisitc mappings. Luo et al. [13] proposed an image encryption algorithm based on double chaotic systems, that is, using two-dimensional Baker chaos graphs to control the system parameters and state variables of logistic chaos graphs. Based on the improved chaotic mapping, a new image encryption algorithm is proposed to improve the security of image encryption. Wang et al. [14] presented a piecewise logistic mapping in four dimensions to the design of a pseudorandom number generator, which is conducive to improving operational efficiency. Wang et al. [15] proposed a new two-dimensional sinusoidal coupled logistic mapping (2D-SCLM), which exhibits superior pseudo-random properties, unpredictability, and a larger chaotic range.

In addition, the chaotic behavior of chaotic systems has important implications for circuit design and optimization, and its unpredictability and sensitivity to initial conditions can be used to enhance circuit functionality in nonlinear systems, offering potential innovations for a variety of electronics applications. The discrete chaotic system is especially suitable for the realization of digital circuits. And, the circuit implementation of chaotic systems has been applied in numerous engineering developments. One of the major applications of chaotic circuits is in the formation of various chaotic secure communication circuits. [16–19] and its application in neural networks [20]. Therefore, the circuit implementation of chaotic mapping is necessary.

In recent years, many new chaotic mappings have been proposed based on traditional chaotic mappings, specifically designed for practical applications, thus expanding the traditional chaotic theory. For example, Tutueva et al. [21] proposed a new method to increase the period length by changing the symmetry coefficients of the adaptive Chirikov mapping, and demonstrated the effectiveness of the proposed method, which can be applied to cryptographic applications and the design of secure communication systems. Alawida et al. [22] introduces a bit reversal approach to enhance digital chaotic mappings by improving their chaoticity, complexity, and statistical properties, demonstrating its effectiveness in a pseudorandom bit generator with strong randomness, uniform distribution, and high key sensitivity. Tutueva et al. [23] achieved the synchronization of the adaptive Hémon mapping by controlling the symmetry coefficients, and applied this method to a communication system based on chaos system switching parameter modulation.

Despite the extensive research and broad applications of the logistic mapping, there remain some limitations, particularly regarding its chaotic characteristics, such as sensitivity to initial conditions, bifurcation behavior, and the range of chaotic states. These constraints hinder its potential in high-performance applications, such as encryption algorithm design, control theory, and pseudorandom number generation. Although previous studies have proposed various modifications to the logistic mapping, such as incorporating fractional-order terms, delayed feedback, and extending the system to higher dimensions, these models either fail to prove their chaotic nature through formal mathematical definitions or focus on specific applications.

The innovation of the piece lies in the introduction of a new mapping form, the piecewise logistic-like mapping (PLLM), which overcomes the limitations of related research on logistic mappings and enhances chaotic characteristics. Most importantly, it rigorously proves that PLLM satisfies the mathematical definition of Devaney chaos. This makes PLLM particularly suitable for applications that require high unpredictability and secure data generation. Furthermore, the simulation of PLLM through circuit design enables its practical application in secure communication circuits.

The arrangement of this article is as follows. In Section 2, a new piecewise logistic-like model is proposed, and its Devaney chaoticity is proved. In Section 3, the basic dynamic properties of the PLLM are studied theoretically and numerically. In Section 4, the PLLM is implemented by analog circuit. Finally, in Section 5, the conclusions and outlook are presented.

2. Piecewise logistic-like mapping

May introduces LM_S, defined as

$$x_{n+1} = \mu x_n(1 - x_n), \tag{2.1}$$

where $\mu \in (0, 4)$ and the initial value $x \in (0, 1)$. Acho et al. [24] presented a one-dimensional logistic-like mapping (LLM) as follow:

$$x_{n+1} = -\mu \mathrm{sgn}(x_n)(1 - x_n), \tag{2.2}$$

where sgn( ) denotes the signum function and $\mu \in (1, 1.4]$.

By improving Eq (2.2), a new definition of PLLM is proposed as follow:

$$x_{n+1} = \begin{cases} \mu(x_n - \frac{1}{4})sgn(x_n - \frac{1}{4}), 0 \le x_n < \frac{1}{2}; \\ \mu(x_n - \frac{3}{4})sgn(x_n - \frac{3}{4}), \frac{1}{2} \le x_n \le 1, \end{cases} \tag{2.3}$$

where $\mu \in (0, 4]$, the initial value $x \in (0, 1)$, and sgn( ) represents the signum function. In this section, the proof of chaos for this PLLM is proved based on the Devaney definition reviewed below.

Definition 1. *(Devaney chaos) ([25]) Let $(\mathcal{X}, d)$ be a metric space. A function $f : \mathcal{X} \to \mathcal{X}$ is called chaotic in the sense of Devaney if it adheres to the three conditions listed below.*

(D1) *f is topological transitive. That is, there exists a $x^* \in \mathcal{X}$ such that $\overline{Orb_f(x^*)} = \mathcal{X}$.*

(D2) *The periodic points of the function f are dense in the space $\mathcal{X}$, where a point x is defined as periodic if there exists a positive integer k for which $f^k(x) = x$.*

(D3) *f is sensitive to initial conditions (briefly sensitive). That is, there exists a $\delta > 0$, for any point $x \in \mathcal{X}$, and for a neighborhood U of x, one can find a point $y \in U$ such that $d(f^k(x), f^k(y)) > \delta$ for some k.*

For convenience, when $\mu = 4$, Eq (2.3) is rewritten as function (2.4) below.

$$f(x) = \begin{cases} 1 - 4x, 0 \le x \le \frac{1}{4}; \\ 4x - 1, \frac{1}{4} < x < \frac{2}{4}; \\ 3 - 4x, \frac{2}{4} \le x < \frac{3}{4}; \\ 4x - 3, \frac{3}{4} \le x \le 1. \end{cases} \tag{2.4}$$

Lemma 1. *The rewritten PLLM* (2.4) *has the following characteristics in binary. For any* $x \in [0,1]$, *represented as a binary pure decimal* $x = 0.a_1a_2a_3\cdots a_m\cdots$, *where* $a_i \in \{0,1\}$,

1) If $a_2 = 0$, *then* $f(x) = 0.\overline{a}_3\overline{a}_4\cdots\overline{a}_m\cdots$;

2) If $a_2 = 1$, *then* $f(x) = 0.a_3a_4\cdots\overline{a}_m\cdots$,

where

$$\overline{a}_m = 1 - a_m = \begin{cases} 0, a_m = 1 \\ 1, a_m = 0 \end{cases} \quad (\forall m \in \mathbb{N}).$$

Proof. Since $x = 0.a_1a_2a_3\cdots a_m\cdots$ is binary notation, then the decimalism of x is $\frac{a_1}{2} + \frac{a_2}{2^2} + \frac{a_3}{2^3} + \cdots + \frac{a_m}{2^m} + \cdots = \sum_{m=1}^{\infty}\frac{a_m}{2^m}$, and according to (2.4), there are four cases:

(i) If $x \in [0, \frac{1}{4})$, then $a_1 = 0, a_2 = 0$. So, x is expressed as a series: $x = \frac{a_3}{2^3} + \frac{a_4}{2^4} + \cdots + \frac{a_m}{2^m} + \cdots$. Thus,

$$f(x) = 1 - 4x = 1 - 4(\frac{a_3}{2^3} + \frac{a_4}{2^4} + \cdots + \frac{a_m}{2^m} + \cdots) = 1 - (\frac{a_3}{2} + \frac{a_4}{2^2} + \cdots + \frac{a_m}{2^{m-2}} + \cdots)$$
$$= \frac{1-a_3}{2} + \frac{1-a_4}{2^2} + \cdots + \frac{1-a_m}{2^{m-2}} = 0.\overline{a}_3\overline{a}_4\cdots\overline{a}_m\cdots.$$

(ii) If $x \in [\frac{1}{4}, \frac{2}{4})$, then $a_1 = 0, a_2 = 1$. That is, x is expressed as a series: $x = \frac{1}{2^2} + \frac{a_3}{2^3} + \frac{a_4}{2^4} + \cdots + \frac{a_m}{2^m} + \cdots$. So,

$$f(x) = 4x - 1 = 4(\frac{1}{2^2} + \frac{a_3}{2^3} + \frac{a_4}{2^4} + \cdots + \frac{a_m}{2^m} + \cdots) - 1 = \frac{a_3}{2} + \frac{a_4}{2^2} + \cdots + \frac{a_m}{2^{m-2}} + \cdots$$
$$= 0.a_3a_4\cdots a_m\cdots.$$

(iii) If $x \in [\frac{2}{4}, \frac{3}{4})$, then $a_1 = 1, a_2 = 0$, i.e., x is expressed as a series: $x = \frac{1}{2} + \frac{a_3}{2^3} + \frac{a_4}{2^4} + \cdots + \frac{a_m}{2^m} + \cdots$. So,

$$f(x) = 3 - 4x = 3 - 4(\frac{1}{2} + \frac{a_3}{2^3} + \frac{a_4}{2^4} + \cdots + \frac{a_n}{2^n} + \cdots) = 1 - (\frac{a_3}{2} + \frac{a_4}{2^2} + \cdots + \frac{a_m}{2^{m-2}} + \cdots)$$
$$= 0.\overline{a}_3\overline{a}_4\cdots\overline{a}_m\cdots.$$

(iv) If $x \in [\frac{3}{4}, 1]$, then $a_1 = 1, a_2 = 1$. So, x is expressed as a series: $x = \frac{1}{2} + \frac{1}{2^2} + \frac{a_3}{2^3} + \frac{a_4}{2^4} + \cdots + \frac{a_m}{2^m} + \cdots$. Thus,

$$f(x) = 4x - 3 = 4(\frac{1}{2} + \frac{1}{2^2} + \frac{a_4}{2^3} + \frac{a_4}{2^4} + \cdots + \frac{a_m}{2^m} + \cdots) - 3 = \frac{a_3}{2} + \frac{a_4}{2^2} + \cdots + \frac{a_m}{2^m} + \cdots$$
$$= 0.a_3a_4\cdots a_m\cdots.$$

By (i) and (ii), if $a_2 = 0$, then $f(x) = 0.\overline{a}_3\overline{a}_4\cdots\overline{a}_m$. By (ii) and (iv), if $a_2 = 1$, then $f(x) = 0.a_3a_4\cdots a_m\cdots$. This completes the proof of Lemma 1. □

Lemma 2. *Let* σ *be the Bernouli shift mapping. For the mapping* $f(x)$, *and any* $n \in \mathbb{N}$, $f^n = f\cdot\sigma^{2(n-1)}$, *where* σ^0 *is the identity mapping.*

Proof. It can be obtained by mathematical induction.

If $n = 1$, then $f\cdot\sigma^{2(1-1)} = f^1$. That is, $f^n = f\cdot\sigma^{2(n-1)}$ is true.

If $n = 2$, for any $x \in [0.1]$, let the binary representation of x be $x = 0.a_1a_2\cdots a_m\cdots$, where $a_i \in \{0,1\}$. Then,

$$f\cdot\sigma^2(x) = f(0.a_3a_4\cdots a_m\cdots) = \begin{cases} 0.\overline{a}_5\overline{a}_6\cdots\overline{a}_m\cdots, a_4 = 0; \\ 0.a_5a_6\cdots a_m\cdots, a_4 = 1. \end{cases} \tag{2.5}$$

Since

$$f(x) = f(0.a_1a_2a_3\cdots a_m\cdots) = \begin{cases} 0.\overline{a}_3\overline{a}_4\cdots\overline{a}_m\cdots, a_2 = 0; \\ 0.a_3a_4\cdots a_m\cdots, a_2 = 1, \end{cases}$$

then

$$f^2(x) = \begin{cases} 0.\overline{a}_5\overline{a}_6\cdots\overline{a}_m\cdots, a_2 = 0, a_4 = 0; \\ 0.a_5a_6\cdots a_m\cdots, a_2 = 0, a_4 = 1; \\ 0.\overline{a}_5\overline{a}_6\cdots\overline{a}_m\cdots, a_2 = 1, a_4 = 0; \\ 0.a_5a_6\cdots a_m\cdots, a_2 = 1, a_4 = 1, \end{cases}$$

i.e.,

$$f^2(x) = \begin{cases} 0.\overline{a}_5\overline{a}_6\cdots\overline{a}_m\cdots, a_4 = 0; \\ 0.a_5a_6\cdots a_m\cdots, a_4 = 1. \end{cases} \tag{2.6}$$

According to (2.5) and (2.6), $f^2 = f \cdot \sigma^2$.

Hypothesis $f^{n-1}{=}f \cdot \sigma^{2(n-2)}$ is true. The following proves $f^n{=}f \cdot \sigma^{2(n-1)}$.

In fact,

$$f \cdot \sigma^{2(n-1)} = [f \cdot \sigma^{2(n-2)}] \cdot \sigma^2 = f^{n-1} \cdot \sigma^2 = f^{n-2}(f \cdot \sigma^2) = f^{n-2} \cdot f^2 = f^n.$$

Thus, $f^n{=}f \cdot \sigma^{2(n-1)}$ for any $n \in \mathbb{N}$.

□

Lemma 3. *([26]) If a dynamical system is transitive, and it has density of periodic points, then it is sensitive to the initial conditions.*

Lemma 4. *([25]) There exists an $x^* \in (0, 1)$ such that arbitrarily given finite sequence "$b_1b_2\cdots b_m$" consisting of 0 and 1 occurred infinitely many times in binary representation of x^*.*

In the following, proceed to verify whether Eq (2.3) satisfies the definition of Devaney chaos. According to Lemma 3, the sensitive dependence on initial conditions in a system defined on a metric space can be deduced from the presence of topological transitivity and density of periodic points. Therefore, it suffices to establish the topological transitivity and the density of periodic points for the PLLM $f(x)$.

Theorem 1. *The periodic points of $f(x)$ are dense in $(0, 1)$. That is, $\overline{\mathrm{Per}(f)} = [0, 1]$ (i.e., for any $x \in [0, 1]$ and any $\varepsilon > 0$, $B(x, \varepsilon) \bigcap \mathrm{Per}(f) \neq \varnothing$), where $\mathrm{Per}(f)$ is the set of all periodic points.*

Proof. For any $x \in [0, 1]$ and any $\varepsilon > 0$, if x is a periodic point of f, then $x \in B(x, \varepsilon) \cap \mathrm{Per}(f) \neq \varnothing$. Suppose $x \notin \mathrm{Per}(f)$. Let $x = 0.a_1a_2\cdots a_m\cdots$, and choose $n \in \mathbb{N}$ such that $\frac{1}{2^{m-1}} < \varepsilon$. Assume x^* is a binary decimal with $a_1a_2\cdots a_{m-1}0$ as its repeating cycle, i.e., $x^* = 0.\dot{a}_1a_2\cdots a_{m-1}\dot{0} \in \mathrm{Per}(f)$. Therefore,

$$|x^* - x| = \left|(0.\dot{a}_1a_2\cdots a_{m-1}\dot{0}) - (0.a_1a_2\cdots a_m\cdots)\right| \leqslant \frac{1}{2^m} + \frac{1}{2^{m+1}} + \cdots = \frac{1}{2^{m-1}} < \varepsilon.$$

Hence, $x^* \in B(x, \varepsilon) \cap \mathrm{Per}(f)$. This implies $\overline{\mathrm{Per}(f)} = [0, 1]$. □

Theorem 2. *The mapping $f(x)$ is transitive, i.e., there exists a $x^* \in (0, 1)$ such that $\overline{Orb_f(x^*)} = [0, 1]$.*

Proof. For any $x \in [0, 1]$, let x be represented as $x = 0.b_1b_2\cdots b_m\cdots (b_i \in \{0, 1\})$. For any $\varepsilon > 0$, select a large enough natural number m to ensure that $\frac{1}{2^m} < \varepsilon$. By Lemma 4, one can select a $x^* \in (0, 1)$ whose binary representation can contain "$b_1b_2\cdots b_m$" infinitely many times.

So, one can construct

$$x^* = 0.a_1^* a_2^* \cdots a_{2(n-1)}^* 01 b_1 b_2 \cdots b_m a_{2(n-1)+m+1}^* \cdots .$$

And,

$$\begin{aligned} |f^n(x^*) - x| &= \left| f \cdot \sigma^{2(n-1)}(x^*) - x \right| = \left| (0.b_1 b_2 \cdots b_m a_{2(n-1)+m+1}^* \cdots) - (0.b_1 b_2 \cdots b_m \cdots) \right| \\ &= \left| (\frac{b_1}{2} + \frac{b_2}{2^2} + \cdots \frac{b_m}{2^m} + \frac{a_{2(n-1)+m+1}^*}{2^{m+1}} + \cdots) - (\frac{b_1}{2} + \frac{b_2}{2^2} + \cdots + \frac{b_m}{2^m} + \cdots) \right| \\ &= \left| \frac{a_{2(n-1)+m+1}^*}{2^{m+1}} + \cdots \cdots \right| \leq \frac{1}{2^{m+1}} + \frac{1}{2^{m+2}} + \cdots = \frac{1}{2^m} < \varepsilon. \end{aligned}$$

Thus, for any $x \in [0, 1]$ and any $\varepsilon > 0$, there exists an $m \in \mathbb{N}$ such that $f^m(x) \in B(x, \varepsilon) = \{y \mid y \in [0, 1] \text{ and } |y - x| < \varepsilon\}$. This implies $\overline{\text{Orb}_f(x^*)} = [0, 1]$. □

In summary, due to the topological transitivity and density of periodic points, the PLLM are chaotic as defined by Devaney.

3. Dynamic properties of the PLLM

This section investigates the dynamic properties of PPLM. The results demonstrate that, in comparison to the LM and the LLM, PPLM exhibits superior performance across several metrics, including sensitivity, permutation entropy, distribution of function sequences, and Lyapunov exponents. These findings highlight its substantial potential for applications in fields such as image encryption, secure communications, and related domains.

3.1. Bifurcation diagram

To observe the dynamic behavior of PLLM numerical simulation analysis of bifurcation diagram of the mapping was carried out on the MATLAB simulation platform, as depicted in Figure 1: (a) bifurcation diagram of LM; (b) bifurcation diagram of LLM; (c) bifurcation diagram of PLLM. With the increase of the parameter μ, the system exhibits period-doubling bifurcations. The parameter range of (a) is $(3.57, 4]$, while the parameter range of (b) is $(1, 1.4]$ and the parameter range of (c) is $(1, 4]$. The comparison of the plots reveals that the range of the PLLM parameters is the widest, and, except for the periodic window at μ=2, there are no windows of period-doubling bifurcations.

3.2. Sensitivity analysis

The randomness of chaotic signal originates from the sensitivity of chaotic system, which is the essence of chaos. The so-called sensitivity means that even if there exists only a minor variation in the initial conditions of the system, it may give rise to completely different results after many iterations, resulting in the phenomenon of the "butterfly effect".

For chaotic mapping, choose two iterative sequences A_n and B_n, where the initial term of the sequence A_n is set to A_0 ($A_0 \in (0,1)$) and the initial value of the sequence B_n is set to $B_0 = A_0 + \varepsilon$ ($B_0 \in (0,1)$), and where ε is a fixed offset. Given a threshold σ, define N as the number of iterations required for the first occurrence of $A_n - B_n > \sigma$. Then, the number of iterations of LM, LLM, and PLLM corresponding

to the first occurrence of separation under different initial values is given. The corresponding result is shown in Figure 2. The horizontal axis represents the initial value, and the vertical axis represents the corresponding number of iterations N.

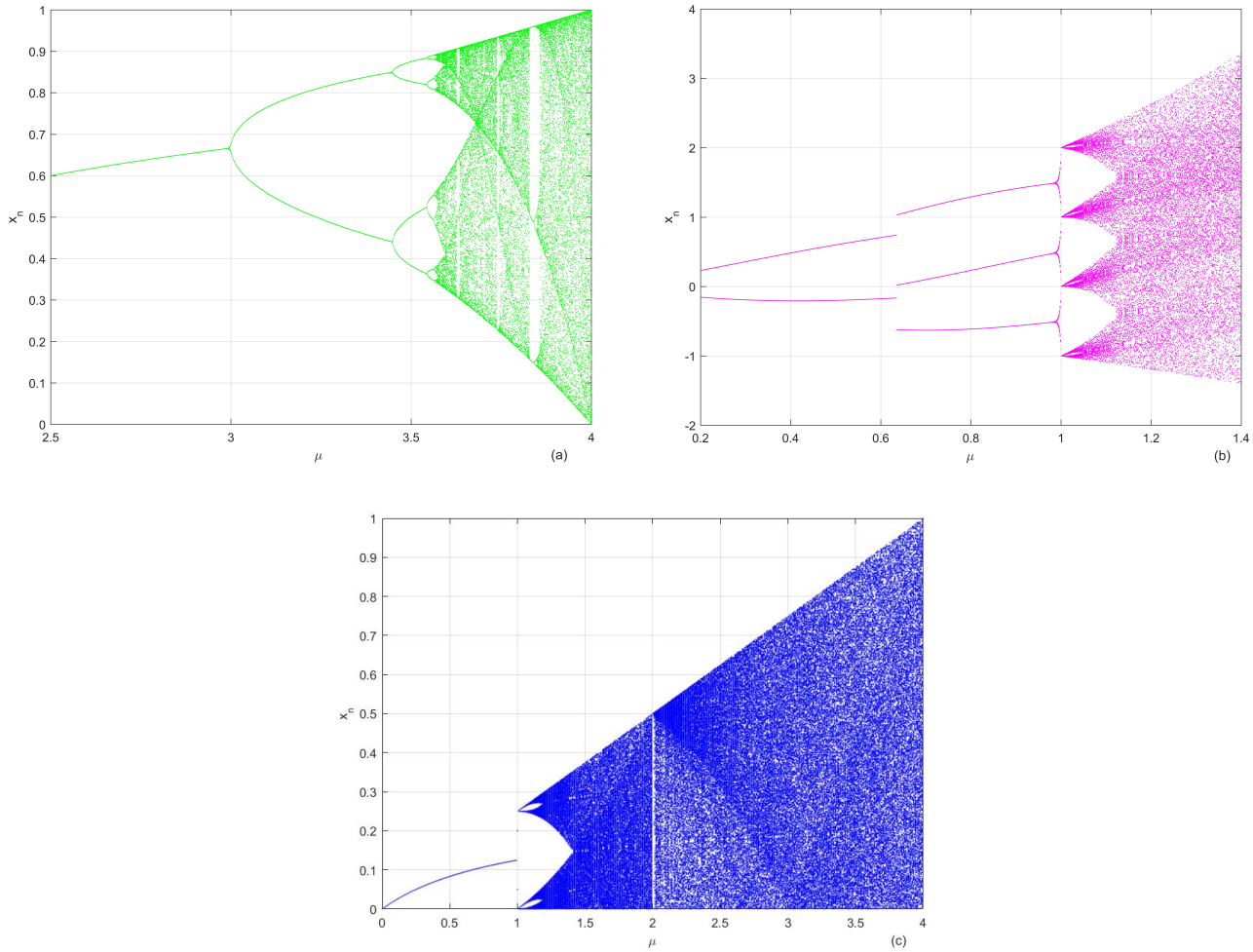

Figure 1. (a) LM bifurcation diagram; (b) LLM bifurcation diagram; (c) PLLM bifurcation diagram.

The difference between two initial values in a chaotic mapping is very small, but after multiple iterations, the gap between the two sequences becomes significantly large, indicating that the mapping exhibits a high sensitivity to initial conditions. Based on the analysis of Figure 2(a)–(c), it can be observed that for any initial value within the interval (0,1), the first separation of LM typically occurs between 15 and 25 iterations, the first separation of LLM occurs between 25 and 28 iterations, and the first separation of PLLM occurs between 8 and 9 iterations. This demonstrates that PLLM has a stronger sensitivity. This property can be leveraged in future studies to design more efficient encryption algorithms.

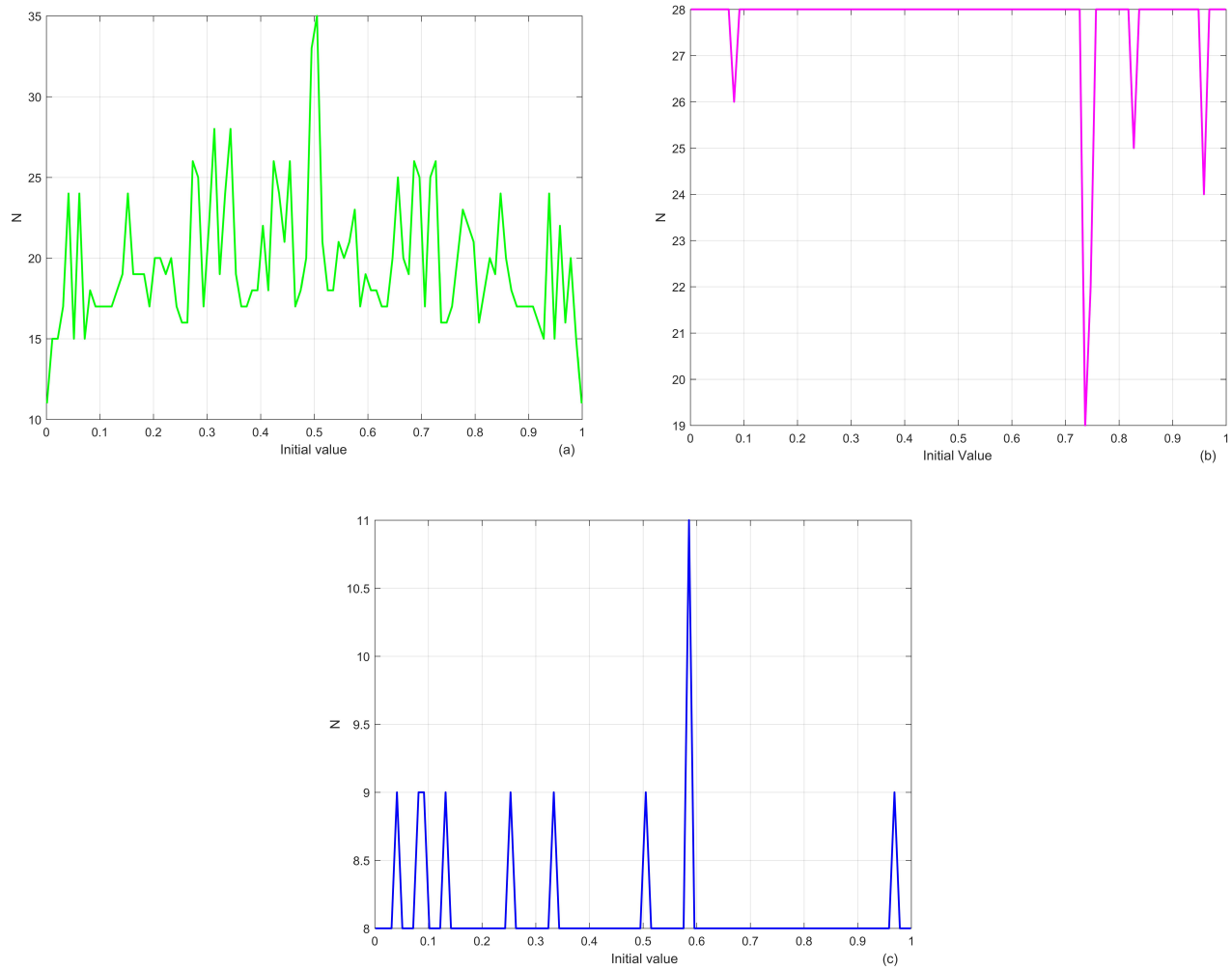

Figure 2. (a) graph of iteration numbers for LM's first separation; (b) graph of iterations numbers for LLM's first separation; (c) graph of iteration numbers for PLLM's first separation.

3.3. Complexity analysis

There are many methods to measure the complexity of chaotic mappings, such as spectrum entropy (SE) [27], C0 entropy [28], permutation entropy (PE) [29], and multiscale permutation entropy (MPE) [30]. Among them, the PE algorithm is the best choice for accurately and quickly estimating the numerical sequence. Therefore, the PE algorithm is used to analyze the PLLM complexity. The larger the value of PE, the more complex the time series [31].

The PE complexity of LM, LLM, and PLLM was calculated under different parameters μ. As shown in Figure 3, for LM in the chaotic regime ($\mu \in [3.6,4]$), the PE complexity remains within the range of [0.6, 0.9]. For LLM in the chaotic regime ($\mu \in [1,1.4]$), the PE complexity stays within the range of [0.52, 0.61]. For PLLM in the chaotic regime ($\mu \in [2,4]$), the PE complexity is maintained within the range of [0.9, 1]. Overall, compared to LM and LLM, PLLM consistently exhibits higher PE complexity. Notably, around $\mu = 2$, PLLM shows a sharp decrease in PE complexity due to the

existence of a periodic window, which is consistent with the bifurcation analysis of PLLM. However, this local decrease does not significantly affect the system's overall high complexity.

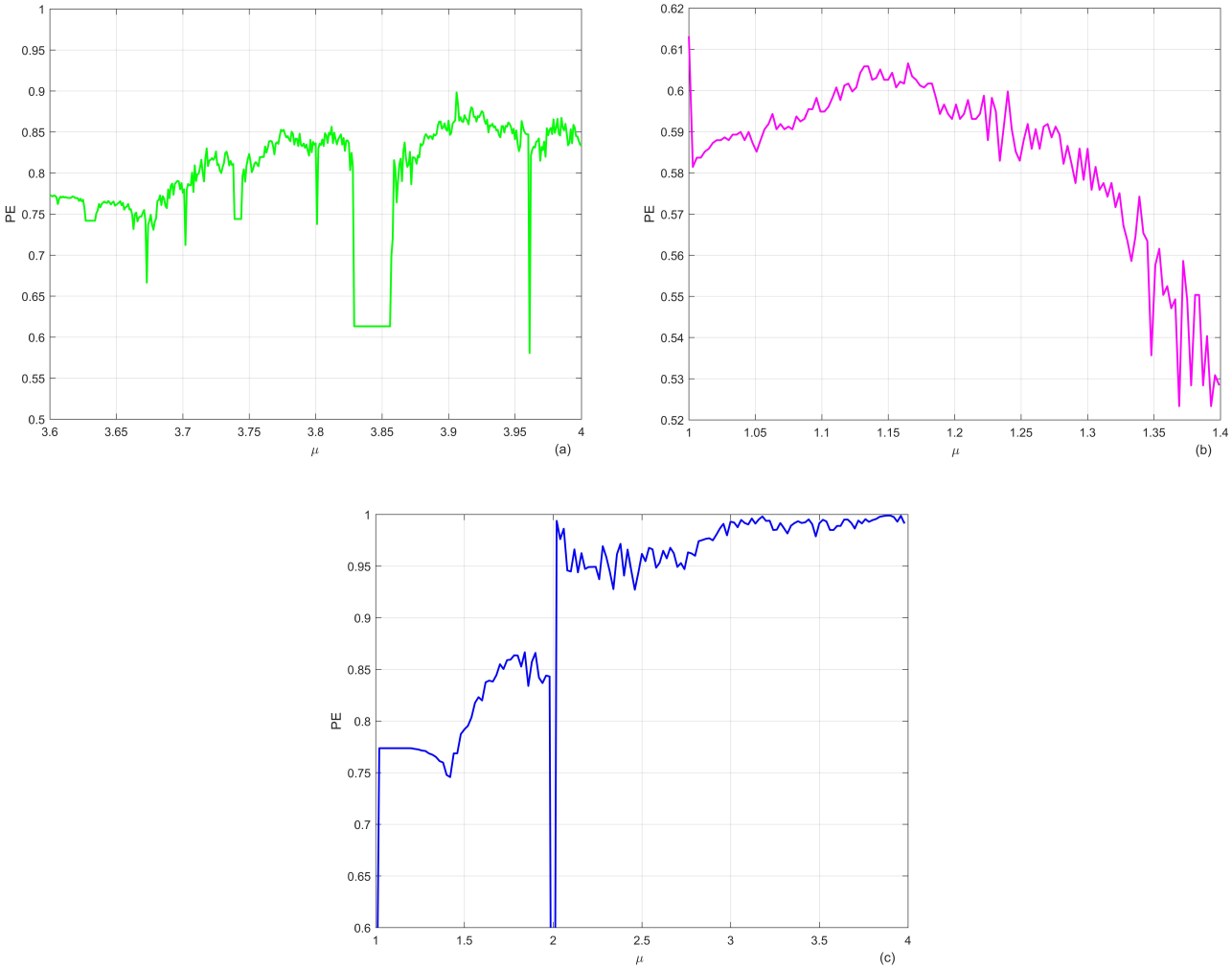

Figure 3. (a) PE complexity of LM; (b) PE complexity of LLM; (c) PE complexity of PLLM.

3.4. Bifurcation iteration count

To further compare the sensitivity of the logistic chaotic mapping and PLLM, we introduce a metric for assessing sensitivity [32]. That is, the bifurcation iteration count of chaotic mappings.

For the chaotic mapping described by $x_{n+1} = f(x_n)$ in Eq (2.3), let the chaotic sequences generated from two distinct initial conditions $c_0 = \{c_1, c_2, \ldots\}$ and $d_0 = \{d_1, d_2, \ldots\}$, respectively. Given a bifurcation threshold δ, define $\Omega = \min\{i : |c_i - d_i| > \delta\}$. Then, Ω is referred to as the bifurcation iteration count for the chaotic mapping $x_{n+1} = f(x_n)$ with initial conditions c_0 and d_0.

Below, we present the average number of iterations necessary for bifurcation corresponding to different bifurcation thresholds for LM, LLM, and PLLM. 5000 points are sampled within the interval $(0, 1)$. And, the average bifurcation iteration count needed to generate chaotic sequences between adjacent points is computed. Table 1 displays the corresponding experimental results.

Table 1. Average number of iterations required for bifurcation in LM, LLM, and PLLM.

Bifurcation Threshold	0.2	0.4	0.6	0.8
LM	11.70	13.02	14.10	18.46
LLM	21.74	23.51	24.32	25.05
PLLM	6.26	7.53	9.42	12.33

The experimental results in Table 1 indicate that, for the same bifurcation threshold value, the average number of iterations required for the LM and LLM are significantly greater than that for the PLLM. That is, the bifurcation speed of the PLLM is faster than that of the LM and LLM, thereby ensuring that the PLLM can enter a chaotic state more quickly during the encryption process.

3.5. Sequential distribution

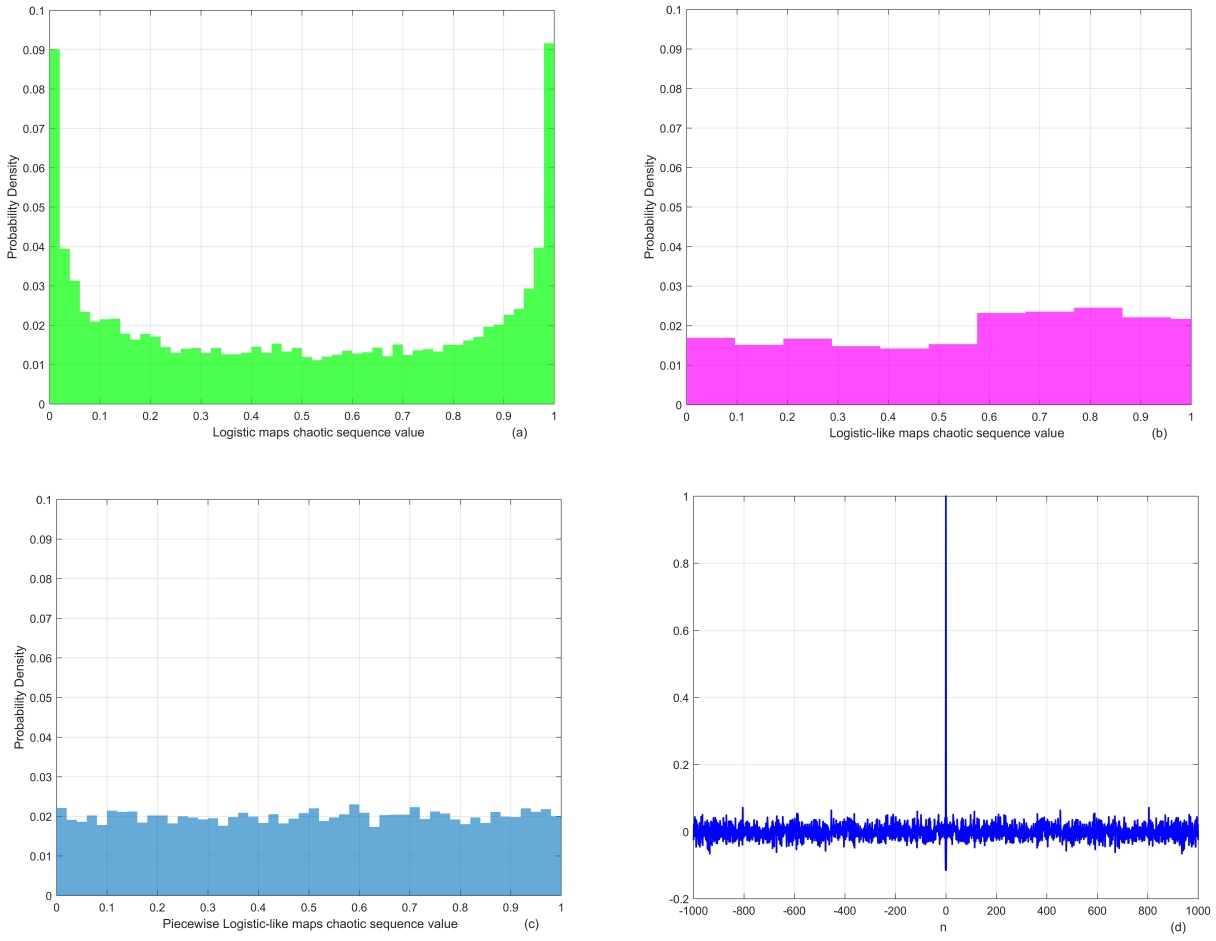

Figure 4. (a) Distribution histogram comparison of the LM sequence; (b) LLM sequence; (c) the PLLM sequence; (d) Autocorrelation function diagram of PLLM.

Next, the randomness of sequences generated by LM, LLM, and PLLM is compared. The distribution of the generated sequence of these three mappings is analyzed experimentally, as shown in Figure

4, where the generated sequence length is 10,000.

As shown in Figure 4(a)–(c), compared with LM and LLM, the sequence distribution histogram of PLLM is more uniform and flat, and there is no logistic mapping distribution peak near 0 and 1, which also indicates that PLLM exhibits better uniformity and randomness. According to Figure 2(d), PLLM has good autocorrelation characteristics, and such chaotic sequences can be utilized as high-quality random number generators. Then, using its uniformity and randomness, data encryption can effectively protect the security of data and resist various attacks. The system can also be applied to specific engineering domains, such as image encryption [33] and chaos-based robot path planning [34].

3.6. Lyapunov exponent

Lyapunov exponents (LE_S) reflect the numerical properties associated with the average exponential divergence of neighboring trajectories in phase space. LE_S are among the features employed to characterize the numerical values of chaotic motion. It is introduced to represent the exponential separation or convergence between adjacent discrete points caused by multiple iterations. LE_S corresponding to the chaotic system $x_{n+1} = f(x_n)$ is defined as

$$\lambda = \lim_{n\to\infty} \frac{1}{n} \sum_{i=1}^{n-1} \ln \left| \frac{\mathrm{d}f}{\mathrm{d}x} \right|_{x=x_i}. \tag{3.1}$$

Lyapunov exponents less than 0 indicates that, after iterative operations under a mapping, neighboring points will eventually converge to a single point, corresponding to a stable fixed point or periodic behavior of the system. Conversely, if the Lyapunov exponents are greater than 0, it implies that neighboring points will be separated through iterative operations under the mapping, leading to locally unstable trajectories in the chaotic system. Therefore, positive Lyapunov exponents can be used to determine whether a system exhibits chaotic behavior. Figure 5 illustrates the Lyapunov exponents for LM, LLM, and PLLM.

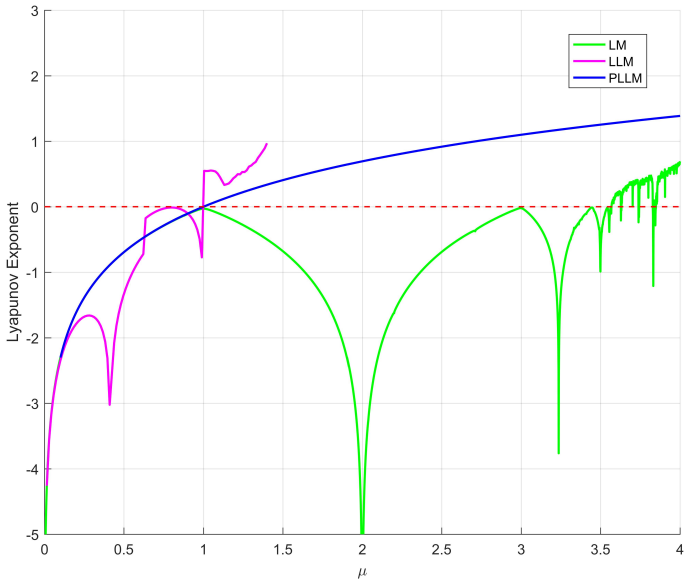

Figure 5. Lyapunov exponential plot of LM, LLM, and PLLM.

For the PLLM,

$$\mathrm{LE}_S = \lim_{N\to\infty} \frac{1}{N} \sum_{k=0}^{N-1} \ln(|f'(x_n;\mu)|). \tag{3.2}$$

However, due to its inclusion of a sign function, it is inherently discontinuous. For the formula PLLM, when the parameter $\mu = 2$, a fixed point appears. From the bifurcation diagram, it can be seen that apart from this point, the system is globally chaotic. Estimating the almost everywhere chaotic nature of such the PLLM can be achieved computationally. To begin with, we will follow the aforementioned procedure. In this instance, one has

$$f(x_n;\mu) = \begin{cases} \mu(x_n - \frac{1}{4})sgn(x_n - \frac{1}{4}), & 0 \le x_n < \frac{1}{2}; \\ \mu(x_n - \frac{3}{4})sgn(x_n - \frac{3}{4}), & \frac{1}{2} \le x_n \le 1. \end{cases} \tag{3.3}$$

Then,

$$f(x_n : \mu) = \begin{cases} -\mu(x_n - \frac{1}{4}), & 0 \le x_n \le \frac{1}{4}; \\ \mu(x_n - \frac{1}{4}), & \frac{1}{4} < x_n < \frac{2}{4}; \\ -\mu(x_n - \frac{3}{4}), & \frac{2}{4} \le x_n < \frac{3}{4}; \\ \mu(x_n - \frac{3}{4}), & \frac{3}{4} \le x_n \le 1. \end{cases}$$

So,

$$f'(x_n;\mu) = \begin{cases} -\mu, & 0 \le x_n \le \frac{1}{4}; \\ \mu, & \frac{1}{4} < x_n < \frac{2}{4}; \\ -\mu, & \frac{2}{4} \le x_n < \frac{3}{4}; \\ \mu, & \frac{3}{4} \le x_n \le 1. \end{cases} \tag{3.4}$$

One can get that $|f'(x_n;\mu)| = \mu > 0$. Thus, LE_S is positive, indicating that the PLLM is almost everywhere chaotic. Contrasting the Lyapunov exponent plots of LM, LLM, and PLLM, one can observe stable chaotic behavior for the LM in the range $3.569946 \le \mu \le 4$ and the LLM in the range $1 \le \mu \le 1.4$. Meanwhile, the PLLM exhibits almost everywhere chaotic behavior across $1 \le \mu \le 4$. The Lyapunov exponents of PLLM is consistently greater than that of LM. Therefore, for PLLM, states with positive LE_S are more prevalent compared to the LM and LLM. This suggests that the constructed PLLM exhibits less stability and faster separation. It poses greater challenges in sequence analysis and prediction.

4. Analog circuit implementation

To validate the physical feasibility of the PLLM introduced in this paper, the following PSIM simulation circuit was designed, as illustrated in Figure 6. The simulation circuit is primarily composed of two parts: (i) an iteration processing circuit, (ii) a discrete mapping circuit. Figure 6 shows the iterative process circuit, which includes two sample-and-hold units, a NOT gate, and two square wave voltage sources. The core of this model is to perform iterative calculations using the sample-and-hold units. Controlled by complementary pulse voltage V_{c1} through the NOT gate, the two sample-and-hold units operate in an inverse phase state, with one sampling while the other holds.

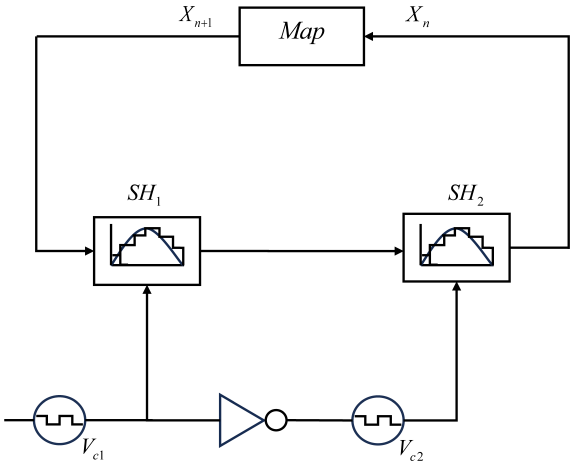

Figure 6. The iterative process circuit.

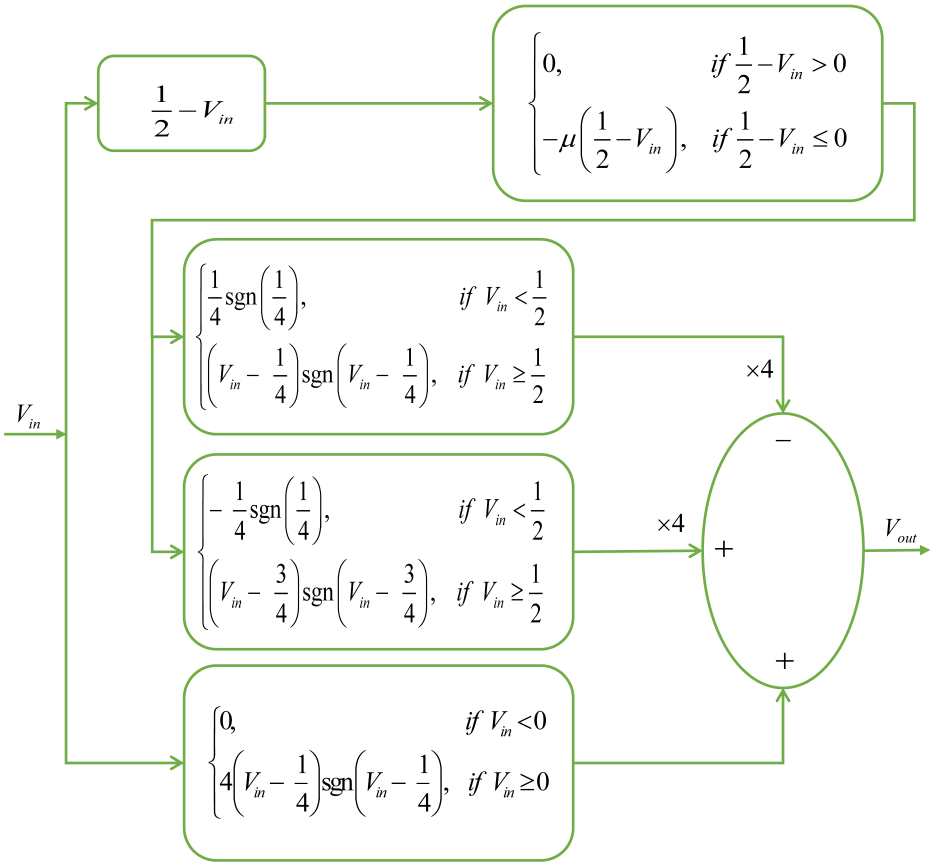

Figure 7. Block diagram of the PLLM circuit diagram.

Figure 7 displays the frame diagram for the PLLM. It consists of an adder, two diodes, three multipliers, three sign function modules, four DC voltage sources, twelve operational amplifiers, twenty-eight resistors, and a sliding potentiometer. Nonlinear terms in the model are realized using multipliers and sign function modules, while the diodes implement the piecewise nature of the analog circuit.

Additionally, operational amplifiers and resistors are used to form the inverting adder.

As shown in Figure 8, this circuit diagram is a schematic diagram of PLLM electronic circuit implementation. Accordingly, the circuit voltage outputs at nodes A–E were analyzed using Kirchhoff's laws.

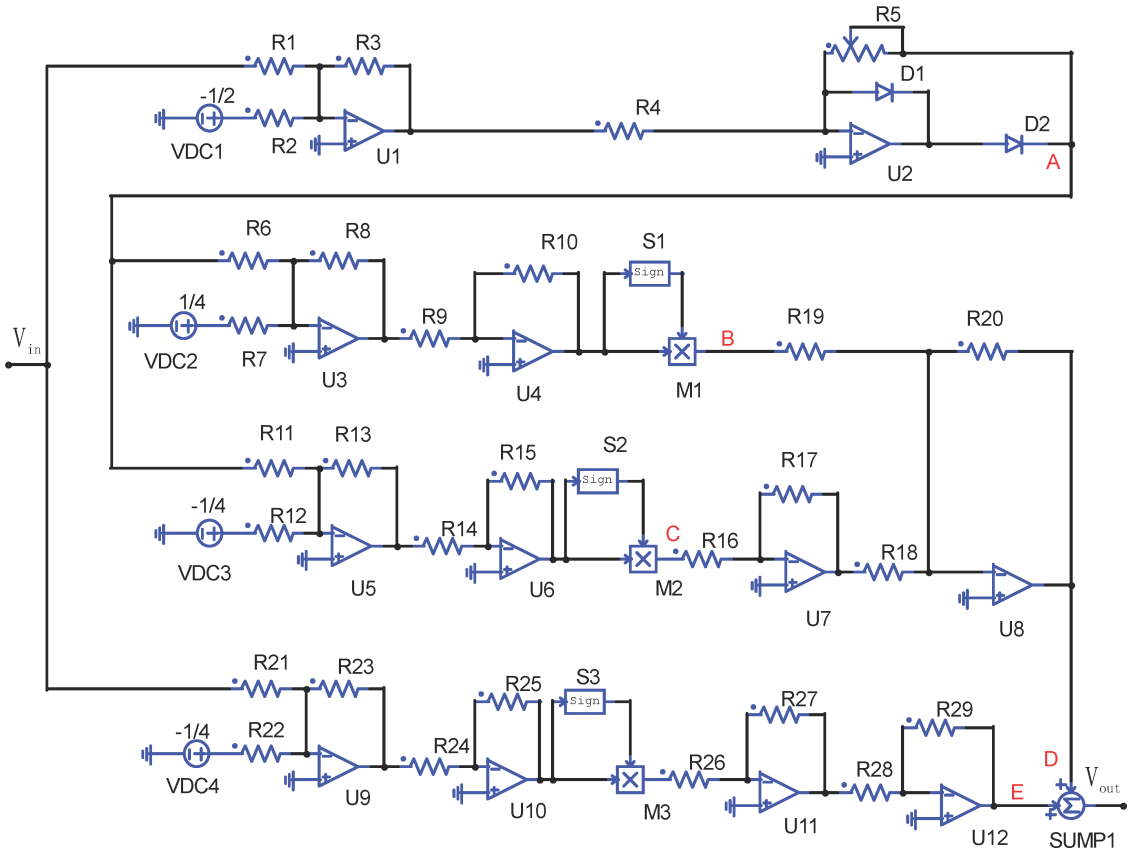

Figure 8. The circuit diagram of the PLLM.

The voltage at node A is provided by the output of the U2 amplifier, which generates a piecewise linear signal.

$$V_A = \begin{cases} 0, & V_{in} < \frac{R_1}{2R_2}; \\ \frac{R_5}{R_4}(\frac{R_3}{R_1}V_{in} - \frac{R_3}{2R_2}), & V_{in} \geq \frac{R_1}{2R_2}. \end{cases} \tag{4.1}$$

The voltages at nodes B and C are provided by the outputs of multipliers M1 and M2, respectively. These signals are derived from the nonlinear modules, yielding the following output voltages V_B and V_C.

$$V_B = (\frac{R_8R_{10}}{R_6R_9}V_A + \frac{R_8R_{10}}{4R_7R_9}) \cdot sgn(\frac{R_8R_{10}}{R_6R_9}V_A + \frac{R_8R_{10}}{4R_7R_9}). \tag{4.2}$$

$$V_C = (\frac{R_{13}R_{15}}{R_{11}R_{14}}V_A - \frac{R_{13}R_{15}}{4R_{12}R_{14}}) \cdot sgn(\frac{R_{13}R_{15}}{R_{11}R_{14}}V_A - \frac{R_{13}R_{15}}{4R_{12}R_{14}}). \tag{4.3}$$

The voltage at node D is given by the output of the U8 amplifier. This signal is then processed

through a subtractor composed of an additional amplifier and resistors, resulting in $4V_C - 4V_B$.

$$V_D = \frac{R_{17}}{R_{16}} \cdot \frac{R_{20}}{R_{18}} V_C - \frac{R_{20}}{R_{19}} V_B. \tag{4.4}$$

The voltage at node E is provided by the output of the U12 amplifier. This signal is obtained through a nonlinear module that utilizes an amplifier, resistors, a multiplier, and a sign function module. The resulting output voltage is

$$V_E = \frac{R_{27}}{R_{26}} \cdot \frac{R_{29}}{R_{28}} \left(\frac{R_{22}R_{25}}{R_{21}R_{24}}\ V_n - \frac{R_{23}R_{25}}{4R_{22}R_{24}}\right) \cdot sgn\left(\frac{R_{22}R_{25}}{R_{21}R_{24}}\ V_n - \frac{R_{23}R_{25}}{4R_{22}R_{24}}\right). \tag{4.5}$$

Finally, the output voltage V_{out} is provided by the output of the adder a1, resulting in $V_D + V_E$. Assuming ideal performance of all components, the state equations of the circuit can be derived as

$$x_{n+1} = \begin{cases} \mu(x_n - \frac{1}{4}) \cdot sgn(x_n - \frac{1}{4}); \\ \mu(x_n - \frac{3}{4}) \cdot sgn(x_n - \frac{3}{4}), \end{cases} \tag{4.6}$$

where x_{n+1} represents the signal V_{out}, and x_n represents the signal V_{in}. The resistance values provided in Table 2 are not unique. Consequently, any values that satisfy Eq (4.6) can be arbitrarily chosen. Based on the analysis above and the component values listed in Table 2, it can be observed that the system exhibits chaotic behavior when $\mu = 4$. Additionally, V_{c1} and V_{c2} are the pulse voltages controlling the sample-and-hold devices, while R_5 is an adjustable variable resistor used to observe different states in the circuit. When implementing chaotic mappings with analog circuits, the discrete time is governed by the input signal pulse voltage V_{c1}. Experimental results of the proposed chaotic system simulation circuit are shown in Figure 9, where the waveforms clearly exhibit discrete states.

Table 2. The values of electronic components in analog circuits for the PLLM.

Device	Value
$R_1, R_2, R_3, R_4, R_6, R_7, R_8, R_9, R_{10}, R_{11}, R_{12}, R_{13}, R_{14}$	
$R_{15}, R_{16}, R_{17}, R_{18}, R_{19}R_{20}, R_{21}, R_{22}, R_{24}, R_{25}, R_{26}, R_{27}, R_{28}$	10 kΩ Resistor
R_{20}, R_{29}	40 kΩ Resistor
R_5	10 kΩ Potentiometer
D1, D2	Diode
U1, U2, U3, U4, U5, U6, U7, U8, U9, U10, U11, U12	Op. Amp
M1, M2, M3	Multiplier
S1, S2, S3	Signum
a1	Adder

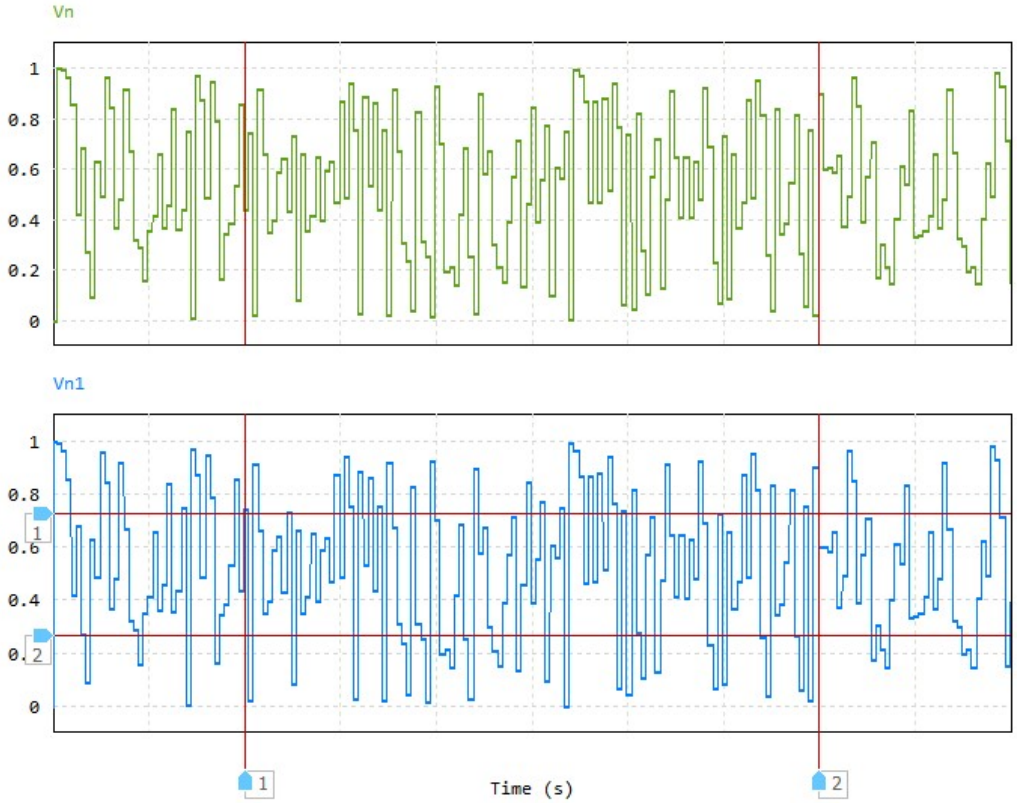

Figure 9. Time series diagram.

5. Conclusions and outlook

Building on the study of the LM, this study proposed an improved PLLM based on the logistic-like mapping introduced in [5]. First, this paper rigorously proves its chaotic behavior theoretically using Devaney's definition of chaos. Then, dynamic behaviors including bifurcation diagrams, Lyapunov exponents, initial value sensitivity, and function sequence distributions, between the PLLM and the LM are compared. The results reveal that the PLLM exhibits more complex dynamic behavior.

Currently, digital technologies are the primary methods for implementing discrete chaotic systems, including DSP (digital signal processors), FPGA (field-programmable gate arrays), and microprocessors. In this paper, an analog circuit is designed to realize the proposed new chaotic mapping using PSIM simulation software. This circuit features a simple structure with a minimal number of component types, offering several potential applications such as random number generation, frequency hopping, and spread spectrum signals. Our next research focus is to incorporate the time series generated by PLLM into the particle swarm optimization (PSO) algorithm to enhance its stochastic detection capability. The improved PSO algorithm will be applied to sensor node positioning optimization in wireless sensor networks.

Use of AI tools declaration

The authors declare they have not used Artificial Intelligence (AI) tools in the creation of this article.

Acknowledgments

This work was funded by Natural Science Foundation of Sichuan Province (No. 2023NSFSC0070), the Opening Project of Sichuan Province University Key Laboratory of Bridge Non-destruction Detecting and Engineering Computing (No. 2024QZJ01), and the Graduate Student Innovation Fundings (No. Y2024334).

Conflict of interest

The authors declare no conflicts of interest regarding the publication of this paper.

References

1. R. M. May, Simple mathematical models with very complicated dynamics, *Nature*, **261** (1976), 459–467. https://doi.org/10.1038/261459a0
2. T. Buchner, J. J. Zebrowski, Logistic map with a delayed feedback: Stability of a discrete time-delay control of chaos, *Phys. Rev. E*, **61** (2000), 016210. https://doi.org/10.1103/PhysRevE.63.016210
3. C. J. Tian, G. Chen, Stability for delayed generalized 2D discrete logistic systems, *Adv. Differ. Equations*, **4** (2004), 1–12. https://doi.org/10.1155/S1687183904308101
4. M. Hénon, A two-dimensional mapping with a strange attractor, *Commun. Math. Phys.*, **50** (1976), 69–77. https://doi.org/10.1007/BF01608556
5. J. C. Sprott, High-dimensional dynamics in the delayed Hénon map, *Electron. J. Theor. Phys.*, **3** (2006), 19–35.
6. G. C. Wu, D. Baleanu, Discrete chaos in fractional delayed logistic maps, *Nonlinear Dyn.*, **80** (2015), 1697–1703. https://doi.org/10.1007/s11071-014-1250-3
7. Y. Wang, Z. L. Liu, J. B. Ma, H. He, A pseudorandom number generator based on piecewise logistic map, *Nonlinear Dyn.*, **83** (2016), 2373–2391. https://doi.org/10.1007/s11071-015-2488-0
8. R. Rak, Route to chaos in generalized logistic map, *Acta Phys. Pol. A*, **127** (2015), 113–117. https://doi.org/10.12693/APhysPolA.127.A-113
9. W. S. Sayed, A. G. Radwan, H. A. H. Fahmy, Design of positive, negative, and alternating sign generalized logistic maps, *Discrete Dyn. Nat. Soc.*, **2015** (2015), 586783. https://doi.org/10.1155/2015/586783
10. G. C. Wu, D. Baleanu, Discrete fractional logistic map and its chaos, *Nonlinear Dyn.*, **75** (2014), 283–287. https://doi.org/10.1007/s11071-013-1065-7
11. E. D. Leonel, E. D. Leonel, The Logistic-Like Map, in *Scaling Laws in Dynamical Systems*, Nonlinear Physical Science, Springer, Singapore, 2021. https://doi.org/10.1007/978-981-16-3544-1_4
12. N. K. Pareek, V. Patidar, K. K. Sud, Image encryption using chaotic logistic map, *Image Vision Comput.*, **24** (2006), 926–934. https://doi.org/10.1016/j.imavis.2006.02.021

13. Y. Q. Luo, J. Yu, W. R. Lai, L. Liu, A novel chaotic image encryption algorithm based on improved baker map and logistic map, *Multimedia Tools Appl.*, **78** (2019), 22023–22043. https://doi.org/10.1007/s11042-019-7453-3

14. Y. Wang, Z. Q. Zhang, G. D. Wang, D. Liu, A pseudorandom number generator based on a 4D piecewise logistic map with coupled parameters, *Int. J. Bifurcation Chaos*, **29** (2019), 1950124. https://doi.org/10.1142/S0218127419501244

15. X. Y. Wang, X. Chen, M. C. Zhao, A new two-dimensional sine-coupled-logistic map and its application in image encryption, *Multimedia Tools Appl.*, **82** (2023), 35719–35755. https://doi.org/10.1007/s11042-023-14674-w

16. A. Kiani-B, K. Fallahi, N. Pariz, H. Leung, A chaotic secure communication scheme using fractional chaotic systems based on an extended fractional Kalman filter, *Commun. Nonlinear Sci. Numer. Simul.*, **14** (2009), 863–879. https://doi.org/10.1016/j.cnsns.2007.11.011

17. M. Halimi, K. Kemih, M. Ghanes, Circuit simulation of an analog secure communication based on synchronized chaotic Chua's system, *Appl. Math. Inf. Sci.*, **8** (2014), 1509. https://doi.org/10.12785/amis/080404

18. R. L. Filali, M. Benrejeb, P. Borne, On observer-based secure communication design using discrete-time hyperchaotic systems, *Commun. Nonlinear Sci. Numer. Simul.*, **19** (2014), 1424–1432. https://doi.org/10.1016/j.cnsns.2013.09.005

19. M. Zapateiro, Y. Vidal, L. Acho, A secure communication scheme based on chaotic Duffing oscillators and frequency estimation for the transmission of binary-coded messages, *Commun. Nonlinear Sci. Numer. Simul.*, **19** (2014), 991-1003. https://doi.org/10.1016/j.cnsns.2013.07.029

20. C. X. Pan, Q. H. Hong, X. P. Wang, A novel memristive chaotic neuron circuit and its application in chaotic neural networks for associative memory, *IEEE Trans. Comput. Aided Des. Integr. Circuits Syst.*, **40** (2020), 521–532. https://doi.org/10.1109/TCAD.2020.3002568

21. A. V. Tutueva, D. Pesterev, A. Karimov, D. Butusov, V. Ostrovskii, Adaptive Chirikov map for pseudo-random number generation in chaos-based stream encryption, in *2019 25th Conference of Open Innovations Association (FRUCT)*, (2019), 333–338. https://doi.org/10.23919/FRUCT48121.2019.8981516

22. M. Alawida, A. Samsudin, J. S. Teh, Enhanced digital chaotic maps based on bit reversal with applications in random bit generators, *Inf. Sci.*, **512** (2020), 1155–1169. https://doi.org/10.1016/j.ins.2019.10.055

23. A. V. Tutueva, L. Moysis, V. G. Rybin, E. E. Kopets, C. Volos, D. N. Butusov, Fast synchronization of symmetric H¨¦non maps using adaptive symmetry control, *Chaos, Solitons Fractals*, **155** (2022), 111732. https://doi.org/10.1016/j.chaos.2021.111732

24. L. Acho, A discrete-time chaotic oscillator based on the logistic map: A secure communication scheme and a simple experiment using Arduino, *J. Franklin Inst.*, **352** (2015), 3113–3121. https://doi.org/10.1016/j.jfranklin.2015.03.028

25. R. Devaney, *An Introduction to Chaotic Dynamical Systems*, CRC press, 1989. https://doi.org/10.4324/9780429502309

26. G. Liu, T. X. Lu, X. F. Yang, W. Anwar, Further discussion about transitivity and mixing of continuous maps on compact metric spaces, *J. Math. Phys.*, **61** (2020), 112701. https://doi.org/10.1063/5.0023553
27. Y. Lin, C. H. Wang, H. Z. He, L. L. Zhou, A novel four-wing non-equilibrium chaotic system and its circuit implementation, *Pramana*, **86** (2016), 801–807. https://doi.org/10.1007/s12043-015-1118-1
28. K. H. Sun, S. B. He, Y. He, L. Z. Yin, Complexity analysis of chaotic pseudo-random sequences based on spectral entropy algorithm, *Acta. Phys.*, **62** (2013), 010501. https://doi.org/10.7498/aps.62.010501
29. C. Bandt, B. Pompe, Permutation entropy: a natural complexity measure for time series, *Phys. Rev. Lett.*, **88** (2002), 174102. https://doi.org/10.1103/PhysRevLett.88.174102
30. W. Y. Dai, X. L. Xu, X. M. Song, G. Li, Audio encryption algorithm based on chen memristor chaotic system, *Symmetry*, **14** (2021), 17. https://doi.org/10.3390/sym14010017
31. X. L. Xu, G. D. Li, W. Y. Dai, X. M. Song, Multi-direction chain and grid chaotic system based on Julia fractal, *Fractals*, **29** (2021), 2150245. https://doi.org/10.1142/S0218348X21502455
32. J. L. Fan, X. F. Zhang, Piecewise logistic chaotic map and its performance analysis, *ACTA Electronica Sinica*, **37** (2009), 720–725, in Chinese. https://doi.org/10.3321/j.issn:0372-2112.2009.04.009
33. G. D. Li, X. L. Xu, H. Y. Zhong, A image encryption algorithm based on coexisting multi-attractors in a spherical chaotic system, *Multimedia Tools Appl.*, **81** (2022), 32005–32031. https://doi.org/10.1007/s11042-022-12853-9
34. T. X. Zhang, H. T. Xing, X. L. Xu, Z. Wang, Y. Zhao, Chaos-based coverage path planning framework for mobile robots and its digital signal processing implementation, *Phys. Scr.*, **99** (2024), 125293. https://doi.org/10.1088/1402-4896/ad8f6e

AIMS Press